



The Performance of Nanofiltration and Electrodialysis on Groundwater Treatment for Mineral Processing

Hugo Guerra¹ · Boris Albijanic¹ · Laurence Dyer¹ · Bogale Tadesse¹

Received: 23 July 2024 / Accepted: 7 November 2024 / Published online: 9 December 2024
© Crown 2024

Abstract

Some resource recovery processes require process water with concentrations of divalent and monovalent ions below 100 mg/L and 500 mg/L, respectively, for optimum performance. This study evaluated the treatment of groundwater from Western Australia with nanofiltration (NF) and electrodialysis (ED) methods to produce fit-for-purpose water for the extractives industry. Various operating conditions such as pressure and voltage were compared. The NF system removed > 95% of divalent cations at the optimum operating conditions, while ED removed > 90% and 98% for monovalent ions (Na^+ and Cl^-) and divalent ions (Ca^{2+} , Mg^{2+} and SO_4^{2-}), respectively. Greater flow rates increased the current density, which decreased the cell performance. The optimum operating conditions for ED were an applied voltage of 1 V per membrane pair, a flux of $2.98 \text{ m}^3 \text{ h}^{-1} \text{ m}^{-2}$, and 40 min of treatment time. The results show that both NF and ED are efficient methods to achieve the quality of water required without exceeding the ion concentration threshold for mineral processing applications. From an economic point of view, ED is the better option due to its low energy consumption and the relatively low replacement costs associated with its high membrane lifetime.

Keywords Water treatment · Extractives · Resource recovery · Membrane technology · Ion removal

Introduction

Australia is ranked 50th among nations with a medium–high risk of experiencing a water crisis, according to estimations from the World Resources Institute's water stress index (Willem et al. 2019). However, with increase in population and growth of the two most significant economic sectors (agriculture and mining), the demand for water is also expected to increase. Looking at the water issue geographically, Western Australia, the Australian state where the mining industry is most concentrated, is one of the driest regions in the world with a limited surface water supply; hence, underground water has become one of the main sources of water for the industry. However, more than 50% of Western Australia's underground water contains salinity > 1500 mg/L (Rioyo 2019).

In many operations around the world, low-quality water with up to 10 times the total dissolved solids (TDS) of

seawater have been used for the extractives industry including in Australia, Indonesia, and South America (Boujounoui et al. 2015). The performance of unit processes such as froth flotation, a common technique for mineral recovery, can be adversely affected by the water quality and TDS, which can eventually result in reduced recovery of valuable minerals (Dzingai et al. 2021; Rankin et al. 2023). The adverse effects of high ion concentrations in water have been linked to the attachment of dissolved ions to mineral surfaces, which decreases the effectiveness of flotation circuits (Boujounoui et al. 2015; Derhy et al. 2020; Zhang et al. 2017). Additionally, it has been shown that the high reactivity of reagents used in the process with salts and the hardness of the water can decrease reagent selectivity and make froth flotation and tailing management operations very difficult (Jung et al. 2022; Manono et al. 2020).

Reverse osmosis (RO) is a membrane separation method often employed for the removal of dissolved species with efficiencies as high as 98% (Wang et al. 2019). However, while being an effective ion removal method, RO inherently consumes high amounts of energy. It becomes an exorbitantly costly water treatment option for many mineral processing activities. Another disadvantage of RO is that the

✉ Bogale Tadesse
bogale.tadesse@curtin.edu.au

¹ Western Australian School of Mines, Curtin University, 95 Egan St, Kalgoorlie, WA 6430, Australia

high percentage of ions removed by this process can cause CaSO_4 scaling, which increases operational cost associated with regular membrane replacement and high doses of anti-scaling chemicals (Muhammad et al. 2022).

With the correct membrane selection and precise conditions, nanofiltration (NF) can offer adequate water quality by eliminating certain monovalent ions and divalent ions (Guerra et al. 2023). NF employs lower transmembrane pressures than RO, which results in cheaper operating costs and less scaling than RO membranes (Jeng and Ron 2019). Most pollutants may be removed from water using NF membranes because of their microporous structure, which can retain particles up to $0.001\ \mu\text{m}$ in size, while lower molecular weight impurities are partially separated in the membrane (Jeng and Rong 2019). Both the size of the pores and the solution-diffusion mechanisms, which are typical mass transfer mechanisms of RO and ultrafiltration, are used in NF to separate the various impurities.

Charged membranes are used to remove ionic species from one solution to another during the electrochemical separation process known as electrodialysis (ED). This method is frequently utilized for producing salt, treating industrial effluents, producing organic acids, recovering usable components from effluents, and producing drinking and process water from brackish and saline water (German et al. 2021). In the ED process, cation and anion exchange membranes alternate between the cathode and the anode, and anions travel towards the anode and cations towards the cathode when a voltage difference exists in the two electrodes. The anion-exchange membranes retain the cations after they have passed through the cation-exchange membranes, which contain sulphone groups on their surface. Meanwhile, the cation-exchange membranes retain the anions, which move via the anion-exchange membranes, which have quaternary ammonium as ion-exchange fixed groups. As a result of this flow of ions, concentrations rise in the concentrate compartment of the cell while falling in the diluate compartment (German et al. 2021; Priyanka et al. 2023).

This study evaluated alternative technologies to RO that can produce water with low ion concentrations suitable for applications in the resource extractive industries. More specifically, NF and ED are promising technologies that use lower pressure and low electrical potential to separate ions across membranes. Hence, this study compared the performance and energy consumption of NF and ED applied to groundwater from the Goldfields area of Western Australia.

Materials and Methods

Materials.

The reagents used for chemical cleaning of the membranes (NaOH and HNO_3), the Na_2SO_4 used as the

electrolyte in the electrode compartments of the ED stack and the NaCl used for synthetic solutions were all analytical grade and were supplied by Chem-Supply, Australia.

The raw water for this study was provided by a mining operation in the Goldfields region of Western Australia, and the characterization of the water is shown in Table 1. Groundwater quality in the Goldfields region ranges from extremely low ($1\ \text{g/L}$ of TDS) to extremely high (up to $250\ \text{g/L}$ of TDS). The groundwater used in this study contained relatively low TDS compared to most of the groundwater in the Goldfields region (Tapley 2017), with the main ions of interest being Mg^{2+} , Ca^{2+} , Na^+ , Cl^- , and SO_4^{2-} .

Methods.

Nanofiltration

Nanofiltration experiments were performed with a pilot-scale rig equipped with a $0.1\ \text{m}^3$ feed tank, a high-pressure booster pump that was used for filtration and for cleaning the membranes, and one pressure vessel housing on a standard $101.6\ \text{cm}$ length \times $10.2\ \text{cm}$ diameter with retractile end caps for the easy changing of the membranes (i.e. Dow Filmtec (NF90 4040) and Ecotechnol (4040 A)). These membranes are characterised as tight NF membranes with relatively high sodium chloride rejection ($> 85\%$). The system was operated at pressures of 8 to 20 bar. The rig was fitted with a pressure gauge to regulate the applied system pressure at the different conditions tested. The brine flow was recycled to the feed tank and the permeate flow was collected in the range of 15 and 65% recoveries. The experimental apparatus is the same as that described in the previous study by the authors (Guerra et al. 2023). Additionally, to maintain the repeatability of the experiments and avoid concentration polarisation, the membranes were chemically cleaned with 0.2% w/w caustic solution.

Table 1 Characterisation of water used in this study showing major impurities

Parameter	Unit	Bore water
pH	–	7.5
Conductivity	$\mu\text{S/cm}$	8280
TDS	mg/L	4150
Cations		
Ca^{2+}	mg/L	140
Mg^{2+}	mg/L	167
Na^+	mg/L	1547
Anions		
Cl^-	mg/L	2340
SO_4^{2-}	mg/L	735

Electrodialysis

Electrodialysis module EDR-Z/2X10-0.8_19 (Membrain) was utilized in this study. This module was fitted with titanium and platinum electrodes and 10 pairs of non-ion selective cation and anion exchange membranes designed for high rates of ion removal. Each membrane pair consisted of one anionic membrane Ralex® AM(H)-PES with an effective surface area of 64 cm² that contained quaternary ammonium as an ion exchange group and one cationic membrane Ralex® CM(H)-PES with an effective surface area of 64 cm² that contained sulphone as an ion exchange group, resulting in a total effective surface membrane area of 1344 cm². A groundwater sample (1 L) was fed to the module through the concentrate and diluate compartments by peristaltic pumps (Master flex L/S) at different flow rates and recirculated in the stack until the desired concentration of ions was achieved in each stream. The effect of the different applied voltages was investigated by adjusting the voltage through a rectifier. A Na₂SO₄ solution (0.15 M) was recirculated through the electrode compartment to avoid electrode reaction and corrosion during experiments. Samples from the diluate were taken at different times to analyse the concentration of ions, conductivity, and TDS.

To maintain reproducibility and avoid concentration polarisation, the ED stack was chemically cleaned before each experiment by a sequence of recirculating 2% NaOH for 30 min, followed by flushing with deionised water, then circulating 2% HNO₃ for 30 min followed by flushing with deionised water.

Chemical Analysis

The analysis of cations such as Ca²⁺, Mg²⁺, Na⁺ was conducted using inductively coupled plasma-optical emission spectroscopy (ICP-OES; Agilent Technologies, Inc., USA) by following the standard method (US. EPA. 2014). Sulphate and chloride concentrations were measured using the standard procedures (APHA 4500 Cl; APHA 4500 SO₄²⁻) and. For the experiment involving NaCl solution, the concentrations of ions in the outlet streams were calculated based on a generated concentration-conductivity calibration curve and the conductivity of the diluate stream was measured with a conductivity meter (Hanna HI98192).

Theory.

Limiting Current Density

The current density in ED can be increased until the ion transfer current exceeds the number of ions available to be transferred; this point is called the limiting current density (LCD). When an ED stack is run at a higher LCD, the process exhibits higher electrical resistance or poorer current

utilization because the ions to be separated at this current level do not have sufficient charge transport capacity, and this is compensated by protons and hydroxyls produced by the hydrolysis of water. Additionally, this can lead to issues like salt precipitation or water dissociation. The limiting current typically depends on the membrane and solution characteristics, the design of the ED stack, and several operational factors including the flow rate of the diluted solution. Therefore, the LCD must be determined to properly run the electrodialyzer. We determined the LCD by measuring the electrical resistance across the membrane stack (Sandra 2011).

Membrane Selectivity in ED

Membrane selectivity (*S*) is a parameter that provides an understanding of ion selectivity by contributing to the knowledge of which ions permeate slower than the others.

$$S_B^A = \frac{CF_A - CF_B}{(1 - CF_A) + (1 - CF_B)} \quad (1)$$

where *CF* is the concentration factor of the ions A and B.

Modelling of ED Systems

Many models have been developed to predict and improve ED operations (Ortiz et al. 2005; Sandra 2011). Typical components of these models include process factors like cell structure, distinctive membrane properties, and operating variables such as voltage and current. In this study, the model and the process were validated using 4.5 g/L NaCl synthetic solution so that the effects of other ions in the process could be neglected.

The following assumptions were made to understand the behaviour of the ED stack used for this specific groundwater treatment. Firstly, convection and ion interaction were not considered while calculating transport because the model was based on the Nernst Planck model. Secondly, the effect of fouling and scaling on the membranes surface were also neglected in this study since small volumes were used and the fluxes were constantly monitored during each experiment to minimise the concentration polarization effect. In addition, the permeability of the membranes was restored by chemical cleaning with caustic solution (0.2% w/w) to restore the membrane's permeability after each experiment to reduce the concentration polarization effect at maximum. Thirdly, it was assumed that the solutions' viscosities would not vary as the ion concentration varied throughout the experiments. Also, the membranes were always considered ideal, so that the cationic membrane was permeable only for cations and the anionic membrane was permeable only to anions. Lastly, the concentrate and diluate tanks and the ED cell were considered perfectly mixed reactors.

In ED, different mass transport phenomena occur inside the stack when current is applied, including the process of ion migration flow (M), where the ion exchange membranes carry the charged species in the solution to the cathode or anode (Ortiz et al. 2005; Sandra 2011).

$$M = \frac{\eta IN}{F} \quad (2)$$

where η is the efficiency of the process calculated from Eq. 3 with the initial and final concentration (C_{initial} and C_{final}), N is the total number of membrane pairs in the stack, I is the current applied, and F is the Faraday constant.

$$\eta = \frac{ZFQ_d(C_{\text{final}} - C_{\text{initial}})}{NI} \quad (3)$$

Another mass transport phenomenon is diffusion flux (D), which is related to the migration of ions due to the gradient in concentration between the concentrate and the diluate, which increases with time.

$$D = \frac{D_{\text{clam}}S}{\sigma_{\text{am}}}(C_{\text{cam}} - C_{\text{dam}})N + \frac{D_{\text{Nacm}}S}{\sigma_{\text{cm}}}(C_{\text{ccm}} - C_{\text{dcm}})N \quad (4)$$

where σ_{cm} and σ_{am} are the cationic and anionic membrane thickness, S is the surface area of membrane, C_{cam} and C_{dam} are the NaCl concentration on the anionic membrane (am) surface in the concentrate and diluate compartment, and C_{ccm} and C_{dcm} are the NaCl concentrations on the cationic membrane (cm) surface in the concentrate and diluate compartments.

$$C_{\text{dam}} = C_{\text{d0}} - \frac{(1 - t_{\text{Cl}^-})\eta I}{FK_m S} \quad (5)$$

$$C_{\text{cam}} = C_{\text{c0}} + \frac{(1 - t_{\text{Cl}^-})\eta I}{FK_m S} \quad (6)$$

$$C_{\text{dcm}} = C_{\text{d0}} - \frac{(1 - t_{\text{Na}^+})\eta I}{FK_m S} \quad (7)$$

$$C_{\text{ccm}} = C_{\text{c0}} + \frac{(1 - t_{\text{Na}^+})\eta I}{FK_m S} \quad (8)$$

where t_{Na^+} and t_{Cl^-} are the transport number of sodium and chloride and K_m is the mass transport coefficient.

In addition to the mass transport equations described above, it was necessary to calculate how the NaCl concentrations in the diluate and concentrate compartments changed with time.

$$NV_{\text{cell}} \frac{dC_{\text{c0}}}{dt} = (C_{\text{ci}} - C_{\text{c0}})Q_c + M - D \quad (9)$$

$$NV_{\text{cell}} \frac{dC_{\text{d0}}}{dt} = (C_{\text{di}} - C_{\text{d0}})Q_c - M + D \quad (10)$$

$$V_{\text{tan k}} \frac{dC_{\text{ci}}}{dt} = (C_{\text{c0}} - C_{\text{ci}})Q_c \quad (11)$$

$$V_{\text{tan k}} \frac{dC_{\text{di}}}{dt} = (C_{\text{d0}} - C_{\text{di}})Q_d \quad (12)$$

where C_{d} and C_{c} are the concentration in the diluate and the concentrate compartments and the sub script “i” and “0” refers to the inlet and the outlet concentrations. As can be seen, the mass balances represent the change in concentration accounting for the migration and diffusion phenomena. Since the mass balance equations are polynomial, the parameters in Table 2 and the function f_{solve} in Matlab was used to solve the system and determine the change in concentration of the diluate with time.

Results and Discussion

Nanofiltration Performance.

Two NF membranes (4040A and NF90 4040) were evaluated under different operating conditions where the rejection (% R_{obs}) of calcium, magnesium, sodium, sulphate, and chloride ions was assessed (Figs. 1 and 2). Both membranes exhibit a similar pattern of ion rejection; as transmembrane pressure rises, so does ion rejection, which is consistent with findings from other studies (Guerra et al. 2023). Figure 1 shows that when the recovery increases, the membrane performance decreases. This is because the concentrate

Table 2 Model parameters used in this study based on data available in the literature

Parameter	Value	References
$D_{\text{Na cm}}$ ($\text{m}^2 \text{s}^{-1}$)	3.28×10^{-11}	[17]
$D_{\text{Cl am}}$ ($\text{m}^2 \text{s}^{-1}$)	3.28×10^{-11}	[17]
K_m (m s^{-1})	0.77×10^{-03}	[17]
η	0.85	
F (C equi^{-1})	96,485	
t_{Na^+}	0.4	[16]
t_{Cl^-}	0.6	[16]
S (m^2)	0.0064	
N	10	
σ_{am} (mm)	0.17	
σ_{cm} (mm)	0.17	

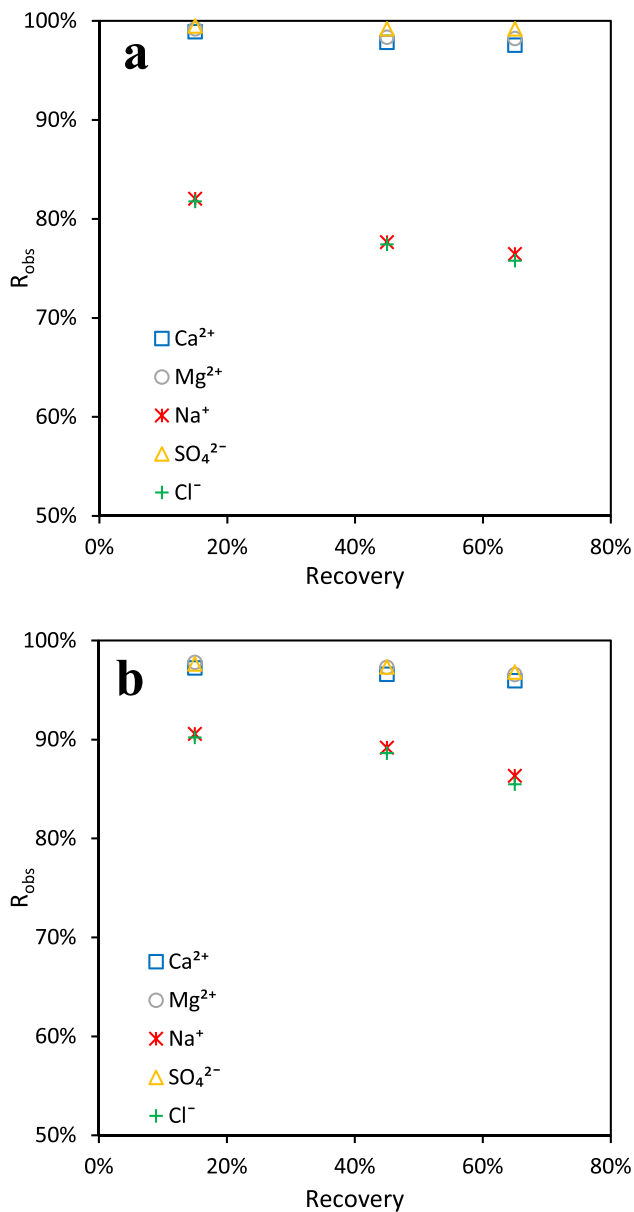


Fig. 1 Effect of water recovery on ion rejection (R_{obs}) at 12 bars. a: NF90 4040 and b: 4040 A

returning to the feed stream raises the ion concentration to be rejected. This in turn increases the ion driving force and alters the properties of the membrane surface, thereby affecting the rejection of ions. However, this pattern was mainly observed in the removal of monovalent ions, which were reduced by 6% and 5% when the water recovery increased from 15 to 65% for the NF90 and 4040A membranes, respectively. On the other hand, the removal of divalent ions was greater than that of the monovalent ions due to hydration energy, since it is more difficult for hydrated divalent ions to permeate through the pores of the membrane, which enhances their retention. As shown in our previous study

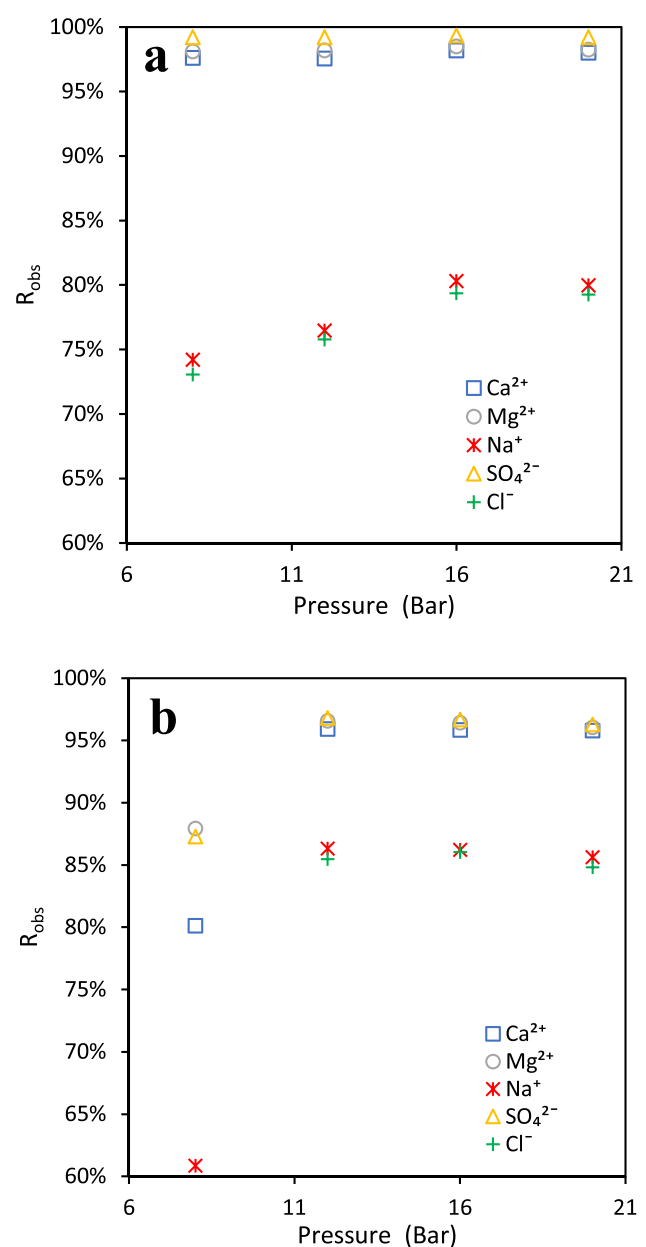


Fig. 2 Ion rejection at different pressure at 65% recovery a: NF90 4040 and b: 4040A

(Guerra et al. 2023), the pore radius of the membranes tested is ≈ 0.29 nm and the ions' respective Stokes radius are 0.31, 0.348, 0.184, 0.231, and 0.121 for Ca^{2+} , Mg^{2+} , Na^{+} , SO_4^{2-} , and Cl^{-} , respectively.

The effect of the transmembrane pressure on ion rejection is shown in Fig. 2. As demonstrated in our previous study, the removal of monovalent ions is affected at high pressures because the mass transfer mechanism is dominated by convection on these specific membranes (Guerra et al. 2023). The membrane rejection processes appear to be governed by the transmembrane pressure, increasing with applied

pressure, and reaching a maximum rejection at > 12 bar of applied pressure. On the other hand, when 8 bar of pressure was applied, the NF90 4040 appeared to strongly reject divalent ions. Figure 2 further demonstrates that at applied pressures > 12 bar and for all examined recovery ranges, the 4040A and NF90 4040 membranes rejected more than 95% of the divalent cations (Ca^{2+} , Mg^{2+}) and more than 74% of the Na^+ . At the same 12 bar of pressure, the evaluated membranes were able to reduce the sulphate and chloride concentrations by 87% and 73%, respectively.

Electrodialysis Performance.

Modelling of a Synthetic NaCl Solution

Figure 3 shows the experimental and theoretical data for the concentration of NaCl in the diluate over time at a current density of 14 A/m^2 . Even though the model was created on an idealised foundation and had numerous restrictions and suppositions, the differences between the experimental and predicted results were small, with an error of 2% during the first two hours of the experiment. However, this error increased up to 14% after that. We attribute most of

this increase in the relative error between the model predictions and the experimental data with time to the assumption of maximum efficiency of the ion permeability of the membranes and parameters assumed from theory not having been measured experimentally. Also, problems of scaling and polarization of the membranes may have contributed to the deviations of the model (Ortiz et al. 2005; Rioyo 2019).

Limiting Current Density

Figure 4 shows the relationship between the limiting current density and V at flow velocities of 2.3 and 4.2 cm/s. Although a plateau was not identified, a change in slope beyond $\approx 1.8 \text{ V}$ and 2.1 V corresponding to the LCDs of 120 A/m^2 and 145 A/m^2 that were observed for the two flow velocities tested (interception dotted lines in Fig. 4). Possible reasons for the absence of the characteristic LCD plateau include the strength of the electric field, the cell's structure, and the turbulence promoters inside the cell, which would all tend to lessen the visibility of the plateau (German et al. 2021; Sandra 2011). The experimental data for the ground-water at two different flow velocities shows that the LCD

Fig. 3 Comparison of experimental and theoretical C_d with ED time for 4.6 g/L NaCl solution

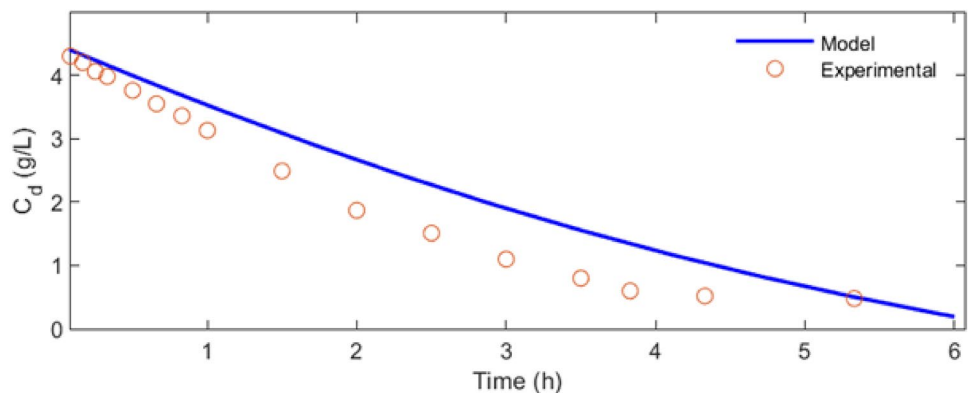
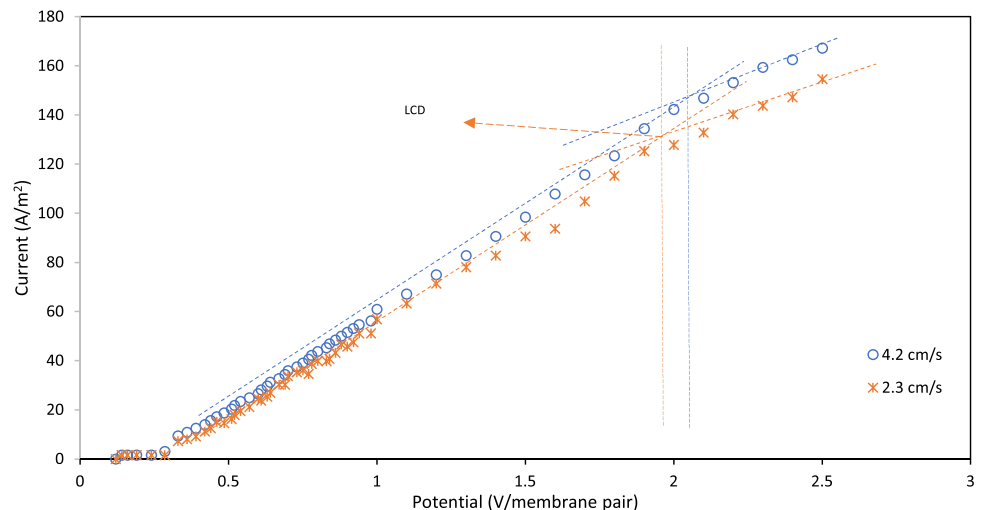


Fig. 4 Limiting current density for bore water at different flow velocities



increases as the flow velocity increases. This is because high flow rates increase turbulence and reduce the thickness of the diffusion layer. This allows electroactive species to move through cells more quickly and reach the membrane surface faster than at low flow velocities. Additionally, because current is proportional to the speed of ion movement, the latter increases at higher flow velocities (German et al. 2021).

Effect of Applied Voltage on Ion Removal

The performance of the ED module was evaluated through the concentration of ions and the change in TDS concentration. The removal of total dissolved ions from the groundwater is shown in Fig. 5. Generally, these are removed faster as higher voltage is applied to the ED stack because of higher current flow and increased movement of ions from the diluate to the concentrate. The desired ion removal is reached faster at higher applied potential and a TDS concentration < 1000 mg/L produced concentrations of < 500 mg/L for monovalent ions such as Na^+ and K^+ and < 100 mg/L for divalent ions such as Ca^{2+} and Mg^{2+} , which are in the suitable range for mineral processing operations (Jung et al. 2022, 2024).

The ion exchange membranes make selective permeation of ions with opposite charges easier, which facilitates the transport of co-ions. Figure 6 shows the depletion of cations and anions from the dilute stream (groundwater) with the applied voltage. As the voltage is increased, the removal of ions is faster because the current flow is increased. At low voltages, such as 0.4 V/membrane pair, divalent and monovalent ions are depleted differently. The depletion rate at 0.4 V/ membrane pair depends on the charge of each ion. Divalent ions such as calcium, magnesium, and sulphate are depleted at a slower velocity than monovalent ions. This is because monovalent ions are less hydrated, making them more susceptible to pull out faster from the diluate. In

addition, the higher the concentration of a specific ion in comparison with the other ions, such as the monovalent ions in the groundwater used in this study, the more it is removed by the membrane. This agrees with the results displayed in Table 3, which show the ion selectivity of the membranes towards the cations and anions at three different voltages. Calcium is transported slower than sodium and magnesium and chloride ions are transported faster than divalent sulphate ions. In addition, the membrane selectivity changes when different voltages are applied. More specifically, when applied voltage is increased, selectivity of the membrane is decreased due to an increase in electrostatic force on the membrane surface, resulting in deposition of monovalent and divalent ions at comparable rates (Nwal et al. 2003; Patel et al. 2020).

Effect of Flow Rate on Ion Removal

The effect of the feed velocity on desalination was evaluated. Figure 7 shows the depletion of TDS on the diluate side and its enrichment in the concentrate stream. TDS analysis shows that, relative to the initial feed concentration, there was a noticeable decrease and increase in TDS from the diluate and concentrate streams, respectively. Comparing a specific point, at 210 min, the reduction of TDS in the diluate at flow velocities of 2.3 and 4.2 cm/s was 82% and 74%, respectively. This suggests that an increase in flow velocity will negatively affect TDS depletion from the diluate to the concentrate stream. This is explained by the shortened residence time of contact between the streams and the membranes. The free movement of ions at low velocities allows the monovalent ions to find exchange sites on the membranes easily, which are usually occupied first by divalent ions that generally impose stronger electrostatic forces (Karimi et al. 2018).

Fig. 5 TDS removal in the diluate stream at different voltages

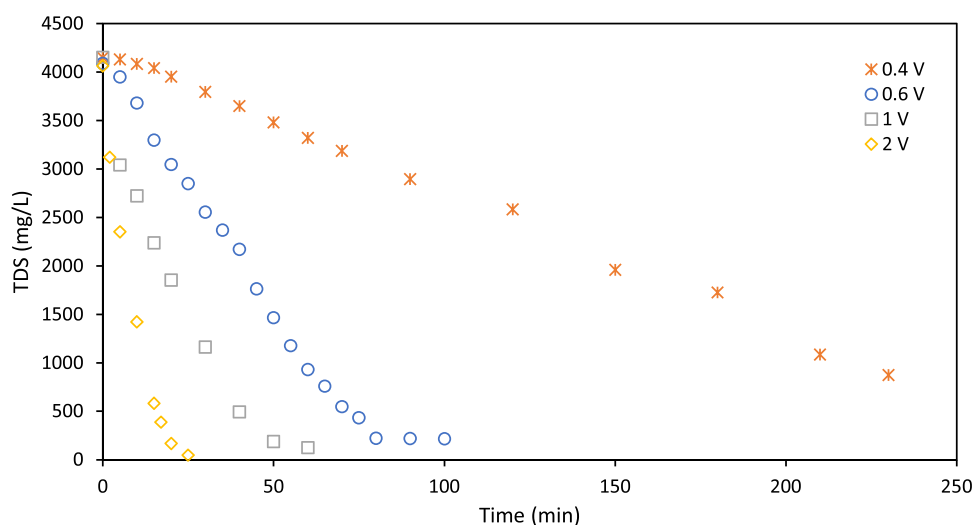


Fig. 6 Effect of voltage per membrane pair on ions removal; a) 0.4, b) 0.6, c) 1, and d) 2 V/membrane

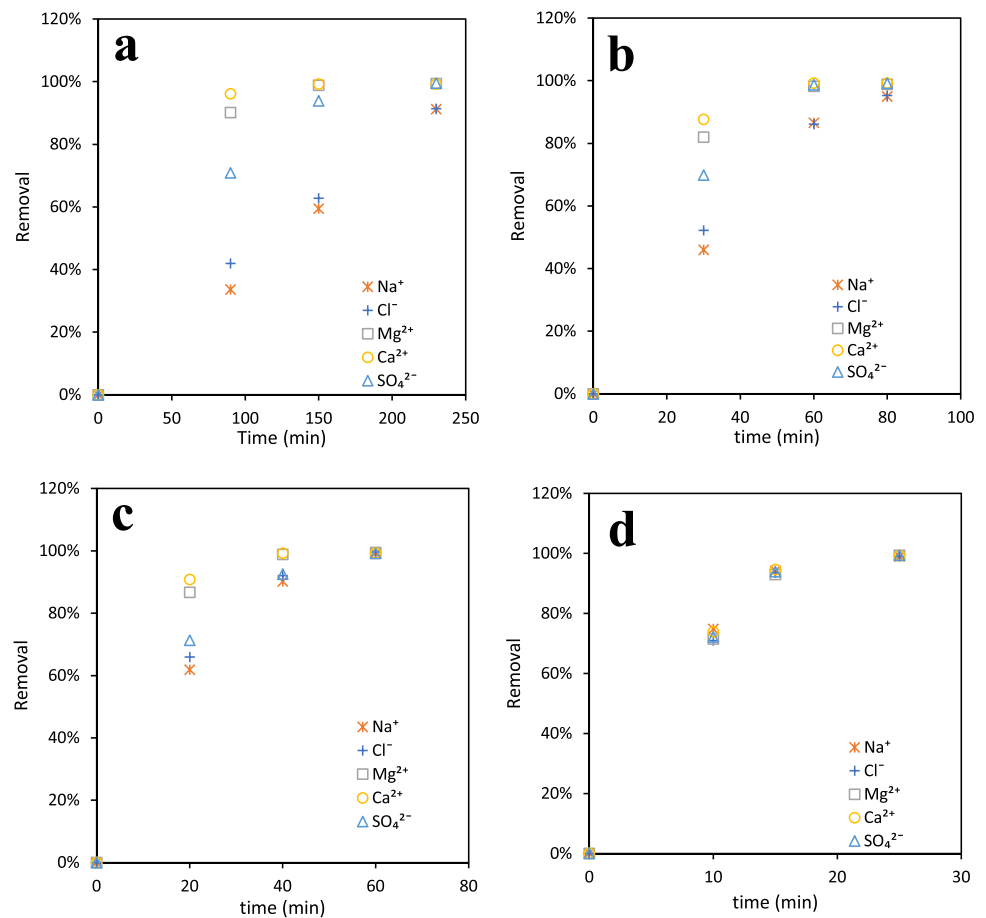


Table 3 ED membrane selectivity towards selected cations and anions

	0.4 V/pair	1 V/pair	2 V/pair
S_{Mg}^{Ca}	-0.00494	-0.00199	-0.000849
S_{Na}^{Ca}	-0.06307	-0.04801	-0.00200
S_{SO4}^{Cl}	0.068325	0.00223	0.002299

Specific Treatment Capacity

Table 4 shows the effect of the applied voltage on treatment capacity for the groundwater used in this study. The findings show that increasing the applied voltage markedly increased the treatment capacity. Systems with a specific treatment capacity > than 30 L/h m² are difficult to operate and require high control and optimisation due to high current densities (PCCell 2023). Based on the characteristics of the water and the results obtained, we found that an applied voltage exceeding 1 V per membrane pair can be complicated to operate.

Energy Cost Estimation.

In membrane processes, energy cost is the main component contributing to operating costs. The high consumption

of energy in processes such as NF and ED is principally associated with the energy consumed in the process of ion mass transfer due to the high voltage and high pressures used in these processes, which could represent up to 60% of the total water treatment cost (Sahu 2021). Specific energy consumption (SEC) can be used to help estimate energy costs.

Electrodialysis

In ED systems, the desalination energy for a specific flow rate is determined by:

$$SEC_{ED} = \frac{U \int_0^t Idt}{Q_{d*} * t} \quad (13)$$

where U is the applied voltage, I is the current, and t is the time to achieve a concentration of TDS below 1000 mg/L (Sosa et al. 2021).

Figure 8 shows the SEC of ED to produce a diluate with an adequate concentration of ions from groundwater tested at a fixed productivity of 14.8 L m⁻² h⁻¹. As expected, the SEC increases exponentially with the number of ions to be depleted from the diluate stream due to the energy required to mobilise ions through the membranes. The

Fig. 7 Effect of feed linear velocity on ion removal

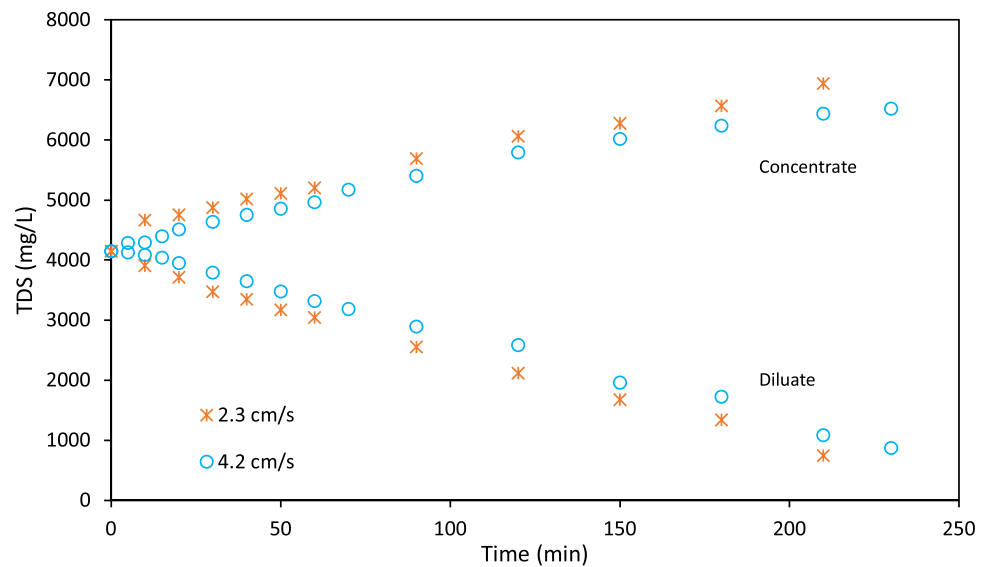


Table 4 Effect of voltage on specific treatment capacity

Applied voltage (V/ membrane pair)	STC (L/h m ²)
0.4	2.13
0.6	7.44
1	14.88
2	37.20

Table 5 Comparison of specific energy consumption and cost

	SEC (kWh/m ³)	\$/ton	References
Nanofiltration	0.523	0.192	This study
	0.68	0.25	[25]
Electrodialysis	0.454	0.167	This study
	0.4–0.5	0.14 – 0.18	[26, 27]

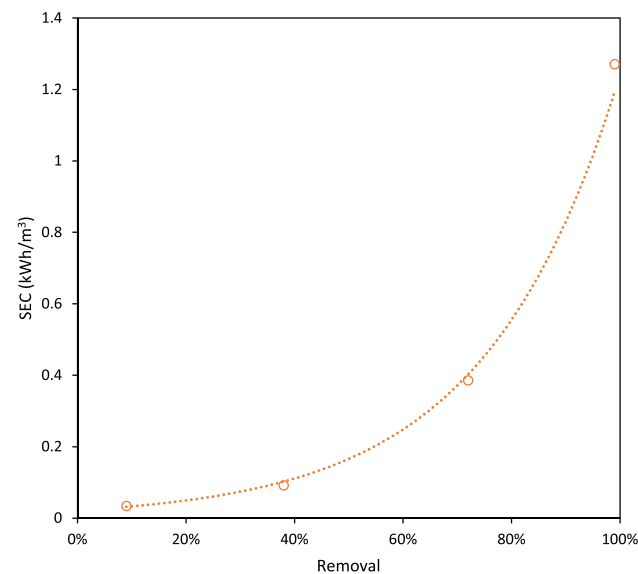


Fig. 8 Effect of feed ions removal on energy consumption

applied voltage results showed that a specific energy consumption of about 0.45 kWh/m³ was needed to achieve 75% TDS removal to generate water within the thresholds

of < 100 mg/L and < 500 mg/L of divalent and monovalent ions, respectively.

Nanofiltration

The specific energy requirements for a pressure-driven process can be quantified by the correlation of the pressure and the recovery of permeate and generally, the energy requirement increases as the pressure of the system increases (Dach 2009). The specific energy consumption of membraned-based water treatment is given by:

$$SEC_{NF} = \frac{\Delta P 100}{\eta r 36} \quad (14)$$

where ΔP is the transmembrane pressure in bar (in this specific study, 12 bar was the pressure at which maximum equilibrium rejection was achieved), η is the global pumping efficiency (generally 85%), and r is the water recovery of the system.

Table 5 compares the SECs for the two best conditions for treating groundwater by NF and ED with the SECs from previous studies where similar operating conditions and feed water were used. For the sake of this comparison, we assumed a standard water consumption of 3 m³ per ton of

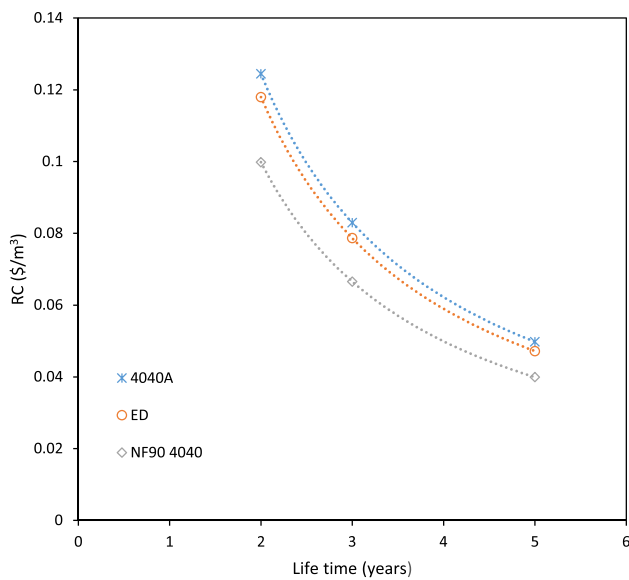


Fig. 9 Membrane replacement cost at different lifetimes for ED and NF systems

ore processed in mineral processing operations, and electricity prices of 0.123 \$/kWh for industry, as reported by the Australian Energy Council in 2022 (Kitchen and Wang 2022; Rankin et al. 2023). In this study, we found that a single stage of NF with 4040A membrane at 12 bar of transmembrane pressure produced water of sufficient quality for mineral separation, at an energy cost of 0.192 \$/ton, while the energy cost to produce water with similar characteristics by ED at 1 V/membrane pair of applied voltage was \approx 0.167 \$/ton, 13% less than NF for this specific groundwater.

Membrane replacement cost is another key operating cost in NF and ED. This variable is associated with the production rate of each membrane and its operational time (lifetime). This parameter can be expressed by the following expression (Nayara et al. 2016; Winston and Sirkar 1992).

$$RC = 2.74F_R M_C M_P^{-1} \quad (15)$$

where RC is the unit replacement cost represented in AUD per every m^3 of water produced at different amounts of membrane lifetime, M_C is the cost of the membrane (AUD/ m^2), which was obtained from a local membrane provider, F_R is the percentage of water recovered, and M_P is membrane productivity (L/ m^2 /day).

The RC estimated for NF and ED based on Eq. 15 is shown in Fig. 9. It is important to note that as the ion rejection increases, the lifetime of the membrane is reduced due to multiple factors such as fouling and concentration polarisation, resulting in an increased driving force (pressure or voltage) to achieve the same results (Govardhan et al. 2020; Liu et al. 2020). The main advantage of ED systems is that

these systems usually provide long lifetimes and depending on the critical ions for each mineral processing operation, the membranes can be perm-selective to monovalent ions. This leads to prolonged lifetimes via reduction of the polarisation by other ions that are not critical (Amshave et al. 2020). Ultimately, the cost optimisation of membrane processes will depend mainly on the driving force of the system and the type of membrane selected to achieve the water quality required.

Conclusions

The resource extractive industry requires large volumes of high purity water, necessitating the use of methods such as reverse osmosis to remove impurities, which has high energy consumption and operational costs. This study examined NF and ED as alternative methods, which under the right conditions of operation and suitable membranes, can potentially be used to treat water with high salinity. In this work, the NF and ED modules produced water with less than 100 mg/L of divalent ions (SO_4^{2-} , Ca^{2+} , and Mg^{2+}), and less than 500 mg/L of monovalent ions (Cl^- and Na^+). In the case of NF, the ion rejection is proportional to the transmembrane pressure. Also, both membranes (NF90 4040, 4040A) rejected more than 95% of the Ca^{2+} and Mg^{2+} and more than 74% of the Na^+ at pressures over 12 bar, with a recovery of 65%. The ED results indicate that ion concentration, linear velocity, and voltage are key to considering ED as an alternative. The optimum ED operating conditions at the flow rate recommended by the manufacturer of 45 L/h is an applied voltage of 1 V per membrane pair where the process can be easily controlled in large-scale operations. At these specific conditions (1 V per membrane pair and 45 L/h) and 40 min of treatment, the removal achieved was more than 90%, 98%, and 87% of monovalent ions (Na^+ and Cl^-), divalent ions (Ca^{2+} , Mg^{2+} , and SO_4^{2-}), and TDS respectively. In terms of energy consumption, ED is 13% more energy efficient than NF. Subtle differences were observed for membrane replacement costs of the two technologies.

Acknowledgements This study was supported by Lynas Rare Earth Ltd and Minerals Research Institute of Western Australia through a Master of Philosophy scholarship at Western Australian School of Mines, Curtin University.

Funding Minerals Research Institute of Western Australia.

References

- Amshave S, Yusri M, Aziz A, Geraint D, Habib I, Abu H (2020) Electrodialysis desalination for water and wastewater: a review. Chem Eng 380:122231. <https://doi.org/10.1016/j.ccej.2019.122231>

- Boujounoui K, Abidi A, Bacaoui A, El Amari K, Yaacoubi A (2015) The influence of water quality on the flotation performance of complex sulphide ores: Case study at Hajar Mine, Morocco. *J South Afr Inst Min Metall* 115(12):1243–1251. <https://doi.org/10.17159/2411-9717/2015/v115n12a14>
- Dach H (2009) Comparing nanofiltration and reverse osmosis processes for selective desalination of brackish water feeds. PhD thesis, Univ D Angers
- Derhy M, Taha Y, Hakkou R, Benzaazoua M (2020) Review of the main factors affecting the flotation of phosphate ores. *Miner* 10:1109. <https://doi.org/10.3390/min10121109>
- Dzingai M, Manono M, Corin K (2021) Probing the effect of water recycling on flotation through anion spiking using a low-grade Cu–Ni–PGM ore: the effect of NO_3^- , SO_4^{2-} and $\text{S}_2\text{O}_3^{2-}$. *Minerals* 11(4):340. <https://doi.org/10.3390/min11040340>
- German D, Alejandra A, Luis L, Maria E, Reyna S, Jesus A (2021) Effect of temperature on diluate water in batch electrodialysis reversal. *Separations* 8:229. <https://doi.org/10.3390/separation8120229>
- Govardhan B, Fatima S, Madhumala M, Sridhar S (2020) Modification of used commercial reverse osmosis membranes to nanofiltration modules for the production of mineral-rich packaged drinking water. *App Water Sci* 10:230. <https://doi.org/10.1007/s13201-020-01312-1>
- Guerra H, Tadesse B, Albijanic B, Dyer B (2023) Nanofiltration for treatment of Western Australian bore water for mineral processing operations: A pilot scale study. *Water Process Eng* 52:103484. <https://doi.org/10.1016/j.wjpe.2023.103484>
- Jeng Y, Rong W (2019) From micro to nano: Polyamide thin film on microfiltration ceramic tubular membranes for nanofiltration. *Membrane Sci* 587:117161. <https://doi.org/10.1016/j.memsci.2019.06.001>
- Jung M, Craig D, Logan A, Dyer L, Albijanic B, Tadesse B (2022) Influence of monovalent and divalent cations on monazite flotation. *Coll Surf A Physicochem Eng Asp* 653:29975. <https://doi.org/10.1016/j.colsurfa.2022.129975>
- Jung M, Tadesse B, Craig D, Logan A, Dyer L, Albijanic B (2024) Understanding the role of water quality in separation of rare earth minerals from iron oxide minerals in a flotation circuit. *Miner Eng* 205:108461. <https://doi.org/10.1016/j.mineng.2023.108461>
- Karimi L, Ghaseemi A, Zamani H (2018) Quantitative studies of electrodialysis performance. *Desalination* 445:159–169. <https://doi.org/10.1016/j.desal.2018.07.034>
- Kitchen C, Wang B (2022) International electricity prices: How does Australia compare? Australian Energy Council
- Liu Y, Zhang Z, Li W, Liu R, Qiu J, Wang S (2020) Water purification performance and energy consumption of gradient nanocomposite membranes. *Composites b: Eng* 202:108426. <https://doi.org/10.1016/j.compositesb.2020.108426>
- Manono M, Corin K, Wiese J (2020) The behavior of gangue during the flotation of a sulfidic PGM-bearing ore in response to various monovalent and divalent ions in process water. *Front Chem* 8(79). <https://doi.org/10.3389/fchem.2020.00079>
- APHA Method 4500-CL: Standard Methods for the Examination of Water and Wastewater. 21 CFR 165.110(b)(4), American Public Health Association
- Muhammad Y, Mai N, Wontae L (2022) Treating reverse osmosis concentrate to address scaling and fouling problems in zero-liquid discharge systems: A scientometric review of global trends. *Sci Total Environ* 844. <https://doi.org/10.1016/j.scitotenv.2022.157081>
- Nayara G, Sundararamana P, O'Connor C, Schacherla J, Heath M, Orozco M, Shaha S, Wright A, Winter A (2016) Feasibility study of an electrodialysis system for in-home water desalination in urban India. *Development Eng* 2:38–46. <https://doi.org/10.1016/j.deveng.2016.12.001>
- Nwal Amang D, Alexandrova S, Schaetzel P (2003) The determination of diffusion coefficients of counter ion and ion exchange membrane using electrical conductivity measurement. *Electrochim* 48:2563–2569. [https://doi.org/10.1016/S0013-4686\(03\)00298-6](https://doi.org/10.1016/S0013-4686(03)00298-6)
- Ortiz J, Sotoca E, Exposito E, Gallud F, Garcia V, Motinel V (2005) Brackish water desalination by electrodialysis: batch recirculation operation modelling. *Membrane Sci* 252:65–75. <https://doi.org/10.1016/j.memsci.2004.11.021>
- Patel S, Qin M, Walker M, Elimelech M (2020) Energy efficiency of electro-driven brackish water desalination: electrodialysis significantly outperforms membrane capacitive deionization. *Environ Sci Tech* 54:3663–3677. <https://doi.org/10.1021/acs.est.9b07482>
- PCCell Complete lab scale systems, control and measurements. Electrodialysis.de. (accessed 15 January 2023)
- Priyanka V, Achlesh D, Kusum A (2023) Development and characterization of novel low-cost engineered pine needle biochar and montmorillonite clay-based proton exchange membrane for microbial fuel cell. *J Water Process Eng* 53. <https://doi.org/10.1016/j.wjpe.2023.103750>
- Rankin P, Kelebek S, Di Feo A, Taylor J (2023) Water recycling and seasonal water quality effects in mineral processing. *Proc*, 61st Conf Metallurgists, Springer, Cham. https://doi.org/10.1007/978-3-031-17425-4_106
- Rioyo J (2019) Integrated treatment of brackish groundwater. Australia Univ of Southern Queensland, PhD Diss
- Sahu P (2021) A comprehensive review of saline effluent disposal and treatment: conventional practices, emerging technologies, and future potential. *J Water Reuse Desalination* 11(1):33–65. <https://doi.org/10.2166/wrd.2020.065>
- Sandra C (2011) Valorization of brines in the chlor-alkali industry. PhD Diss, Univ Politecnica de Catalunya, Spain, Integration of precipitation and membrane processes
- Sosa P, Loc T, Torres M, Tedesco M, Post J, Brunnin H, Rijnaarts H (2021) Energy consumption of an electrodialyzer desalinating aqueous polymer solutions. *Desalination* 510:115091. <https://doi.org/10.1016/j.desal.2021.115091>
- Tapley B (2017) Improving gold mining economics through the use of membrane technology – A study into the reduction of lime and cyanide consumption at WA gold mines. *Ecotechnol MetFest U.S. EPA*. (2014) Method 6010D (SW-846): Inductively Coupled Plasma-Atomic Emission Spectrometry. Revision 4. Washington, DC., accessed July 2024.
- Wang Y, Guo X, Bai Y, Sun X (2019) Effective removal of calcium and magnesium sulfates from wastewater in the rare earth industry. *R Soc Chem* 9:33922–33930. <https://doi.org/10.1039/C9RA05615G>
- Willem R, Reig P, Schleifer L (2019) 17 countries, home to one-quarter of the world's population, face extremely high-water stress. World Resources Institute.
- Winston W, Sirkar K (1992) *Membrane Handbook*. Springer Science+Business Media, New York
- Zhang W, Honaker R, Groppo J (2017) Flotation of monazite in the presence of calcite part I: Calcium ion effects on the adsorption of hydroxamic acid. *Miner Eng* 100:40–48. <https://doi.org/10.1016/j.mineng.2016.09.020>